# *Mex3c* regulates insulin-like growth factor 1 (IGF1) expression and promotes postnatal growth

Yan Jiao, Colin E. Bishop, and Baisong Lu
Institute for Regenerative Medicine, Wake Forest University Health Sciences, Winston-Salem, NC 27157

**ABSTRACT** **Insulin-like growth factor 1 (IGF1) mediates the growth-promoting activities of growth hormone. How *Igf1* expression is regulated posttranscriptionally is unclear. *Caenorhabditis elegans* muscle excess 3 (MEX-3) is involved in cell fate specification during early embryonic development through regulating mRNAs involved in specifying cell fate. The function of its mammalian homologue, MEX3C, is unknown. Here we show that MEX3C deficiency in *Mex3c* homozygous mutant mice causes postnatal growth retardation and background-dependent perinatal lethality. Hypertrophy of chondrocytes in growth plates is significantly impaired. Circulating and bone local production of IGF1 are both decreased in mutant mice. *Mex3c* mRNA is strongly expressed in the testis and the brain, and highly expressed in resting and proliferating chondrocytes of the growth plates. MEX3C is able to enrich multiple mRNA species from tissue lysates, including *Igf1*. *Igf1* expression in bone is decreased at the protein level but not at the mRNA level, indicating translational/posttranslational regulation. We propose that MEX3C protein plays an important role in enhancing the translation of *Igf1* mRNA, which explains the perinatal lethality and growth retardation observed in MEX3C-deficient mice.**

**Monitoring Editor**
A. Gregory Matera
University of North Carolina

Received: Nov 29, 2011
Revised: Feb 14, 2012
Accepted: Feb 17, 2012

## INTRODUCTION

Insulin-like growth factor 1 (IGF1) is a prime mediator of the growth-promoting effects of growth hormone (GH; Rodriguez *et al.*, 2007), which promotes postnatal growth through stimulating endocrinal and local production of IGF1 (Ohlsson *et al.*, 2009). The liver produces 75% of circulating IGF1 in the bloodstream. Eliminating hepatic production of IGF1 in mice does not affect postnatal growth, indicating that 25% of normal circulating IGF1 is sufficient for normal postnatal growth (Sjogren *et al.*, 1999; Yakar *et al.*, 1999; Stratikopoulos *et al.*, 2008). Local production of IGF1 in developing bone is also essential for normal postnatal growth. Chondrocyte- or osteoblast-specific knockout of *Igf1* in mouse causes postnatal growth retardation, although the manipulation does not affect circulating IGF1 levels (Govoni *et al.*, 2007a, 2007b).

Humans and mice have multiple forms of *Igf1* transcripts because of the usage of different polyadenylation sites; some have a short 3′ untranslated region (3′ UTR) of 150~400 nucleotides (nt) (e.g., mouse NM_184052 and human NM_001111285), but some have a long 3′ UTR of more than 6000 nt (e.g., mouse NM_010512 and human NM_001111283). Polysome association analysis found that, of the liver *Igf1* mRNAs with different lengths of 3′ UTR, only the short species were found on polysomes, suggesting that some aspect of the long 3′ UTR may prevent translation (Foyt *et al.*, 1991). Whereas the liver expresses more *Igf1* transcripts with a short 3′ UTR (Bell *et al.*, 1986), bone-forming cells predominantly express *Igf1* transcripts with a long 3′ UTR (Delany and Canalis, 1995). Recently it was found that nocturnin regulates *Igf1* mRNA stability through binding to its 3′ UTR (Kawai *et al.*, 2010). It remains unclear how the translation of *Igf1* mRNA, especially in transcripts with a long 3′ UTR, is regulated.

*Caenorhabditis elegans* muscle excess 3 (MEX-3) is a heterogeneous nuclear ribonucleoprotein (hnRNP) K homology (KH) domain-containing RNA binding protein. It is involved in cell fate specification in the early embryonic stage of *C. elegans* and in the maintenance of the totipotency of the germ line in adult worms (Draper *et al.*, 1996; Hunter and Kenyon, 1996; Ciosk *et al.*, 2006). MEX-3 is thought to prevent the translation of *pal-1* and nanos mRNA in the anterior blastomeres or germ cells

This article was published online ahead of print in MBoC in Press (http://www.molbiolcell.org/cgi/doi/10.1091/mbc.E11-11-0960) on February 22, 2012.

Address correspondence to: Baisong Lu (blu@wakehealth.edu).

Abbreviations used: AA, amino acids; β-gal, β-galactosidase; ELISA, enzyme-linked immunosorbent assay; GH, growth hormone; IGF1, Insulin-like growth factor 1; hnRNP, heterogeneous nuclear ribonucleoprotein; KH domain, hnRNP K homology domain; MEX-3, muscle excess 3; Mex3c, mex3 homologue C (*Caenorhabditis elegans*); MRE, MEX-3 recognition element; nt, nucleotides; qRT-PCR, quantitative RT-PCR; 3′ UTR, 3′ untranslated region; ZNF domain, zinc finger domain.

(Draper *et al.*, 1996; Hunter and Kenyon, 1996; Jadhav *et al.*, 2008). Human and mouse genomes encode four MEX-3 homologues, named MEX3A, MEX3B, MEX3C, and MEX3D (Buchet-Poyau *et al.*, 2007). They all have two KH RNA-binding domains in the N termini which are believed to bind RNA molecules, and a zinc finger (ZNF) domain at the C termini which is believed to mediate protein–protein interactions. MEX3D, once described as TINO, is a *BCL2* mRNA AU-rich element-binding protein and negatively regulates the stability of *BCL2* mRNA (Donnini *et al.*, 2004).

MEX3C (once called RKHD2) is highly conserved among mammalian species. Mouse MEX3C (464 amino acids [AA] according to DDBJ Accession Number BR000945) is 99% identical with human, chimpanzee, and bovine MEX3Cs. A combination of sibling-pair linkage analysis and case–control association studies suggests a contribution of *MEX3C* to the genetic susceptibility of hypertension, although a possible mechanism is unknown (Guzman *et al.*, 2006). So far, no mRNA targets have been reported for MEX3C, and little is known about its role in RNA metabolism.

In our effort to generate rodent mutants for reproductive biology using a Sleeping Beauty transposon-mediated mutagenesis strategy (Lu *et al.*, 2007), we encountered a mutant line with postnatal growth retardation. DNA analysis found three transposon insertions: two in the regions without genes and one in the intron of *Mex3c*. To eliminate the possible influence of transposons outside the *Mex3c* gene, we generated a new *Mex3c* mutant line from a gene trap embryonic stem cell line (Skarnes *et al.*, 2004). Here we show that *Mex3c* plays an important role in promoting postnatal growth, possibly through translational regulation of *Igf1* mRNA.

## RESULTS

### Background-dependent postnatal lethality of *Mex3c* mutant mice

*Mex3c* mutant mice were generated from a gene trap ES cell line, where the *Mex3c* gene was mutated by gene trapping. Based on the National Center for Biotechnology Information (NCBI) EST sequence CJ072395.1 and the mRNA sequence BC125427, the mouse *Mex3c* gene contains three exons, with CJ072395.1 spanning exons 1 and 2, and BC125427 spanning exons 2 and 3. This *Mex3c* mRNA transcript is predicted to encode a protein of 464 AA, containing two hnRNP KH RNA-binding domains (Grishin, 2001) and one ZNF domain (Figure 1A). The NCBI mouse *Mex3c* reference sequence NM_001039214.4 regards intron 1 in Figure 1A as exon sequences, resulting in a protein with an extra 189 AA at the N terminus. In our gene trap mouse, the trapping vector pGT1xrT2 was integrated into the second intron of *Mex3c* (Figure 1B). Reverse transcription PCR (RT-PCR) and DNA sequencing analyses revealed that most transcripts from the trapped allele (written as "tr" hereafter) contained the *LacZ* cDNA from the trapping vector, but lacked the third exon of *Mex3c*, producing a peptide containing the N-terminal 56 AA of the 464 AA MEX3C and the full-length β-galactosidase (β-gal) peptide. Because this fusion peptide lacks the hnRNP KH RNA-binding and the ZNF domains, it is expected to be nonfunctional. The β-gal moiety in the fusion protein permits tracing of the expression of *Mex3c* mRNA through detecting β-gal activity.

Transcripts from the trapped allele, however, also included a low percentage of intact full-length *Mex3c* mRNA due to alternative splicing. Quantitative RT-PCR (qRT-PCR) revealed that authentic *Mex3c* mRNA in +/tr and tr/tr mice comprised ~55% and 2.2% of that of +/+ mice, respectively (Figure 1C). Thus tr/tr mice were not *Mex3c* null but expressed <5% of normal levels of *Mex3c* mRNA. Because neither customized nor commercially available anti-MEX3C antibodies were specific enough to detect endogenous MEX3C protein, the expression level of MEX3C protein in mutant mice is unclear.

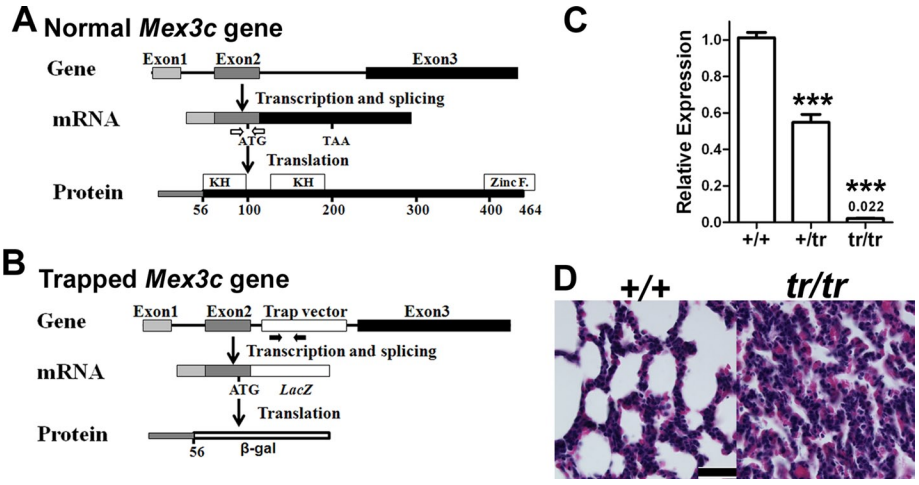


FIGURE 1: Mutation of *Mex3c* in mouse by gene trapping. (A) Structure of normal *Mex3c* gene and its gene products. The black line indicates the introns of mouse *Mex3c* gene, and the solid boxes indicate the three *Mex3c* exons. Exons 2 and 3 contain coding regions. The N-terminal KH RNA-binding domains (KH) and the C-terminal ZNF domain (zinc F) are indicated. The gene structure is based on NCBI EST sequence CJ072395.1 and mRNA sequence BC125427, and is submitted to DDBJ (DNA Data Bank of Japan) with accession number BR000945. Positions of primers used to amplify authentic *Mex3c* mRNA (*Mex3cF* and *Mex3cR*) are indicated by two unfilled arrows. (B) Structure of the trapped *Mex3c* allele and its gene products. The empty box indicates the gene trap vector containing *lacZ* cDNA. The transcript from the trapped allele translates into a peptide containing the N-terminal 56 AA residues from MEX3C and the full-length β-gal. Positions of primers used to amplify the gene trap vector DNA (*TrapF* and *TrapR*) are indicated by two solid arrows. (C) qRT-PCR comparison of authentic *Mex3c* mRNA levels in +/+, +/tr, and tr/tr mice (n = 3 mice for each genotype). Means ± SEM are presented. *** $p < .001$ by Tukey post hoc tests following analysis of variance. Total RNA was isolated from hypothalami. (D) Mutant mice have poorly expanded alveoli after birth. Shown are lung sections of 1-d-old pups stained with hematoxylin and eosin. Scale bar: 50 μm.

Trapping both alleles of the *Mex3c* gene did not affect embryonic development, because the tr/tr pups from +/tr × +/tr matings were born normal with Mendelian ratios. Postnatal survival, however, was affected to variant degrees depending on background. Under a C57BL/6 background, more than 85% of mutants died within several hours after birth. Only seven homozygous mutant mice from more than 160 pups of heterozygous parents survived to weaning time. Mutant pups most likely died from poor breathing, and their bodies were cyanotic. On histological analysis, alveolar spaces in lungs from mutant mice were poorly expanded (Figure 1D). Other primary pulmonary defects were not detected.

*Mex3c*, as assessed by tracing β-gal activity in organs of 1-d-old pups, was highly expressed in muscle (Figure 2A) and multiple internal organs such as the lung and the spleen (Figure 2B). *Mex3c* is expressed at low levels in the liver, and β-gal activity was seen in blood vessel cells but not hepatic cells on liver sections (unpublished data). Because of the important roles of the lung

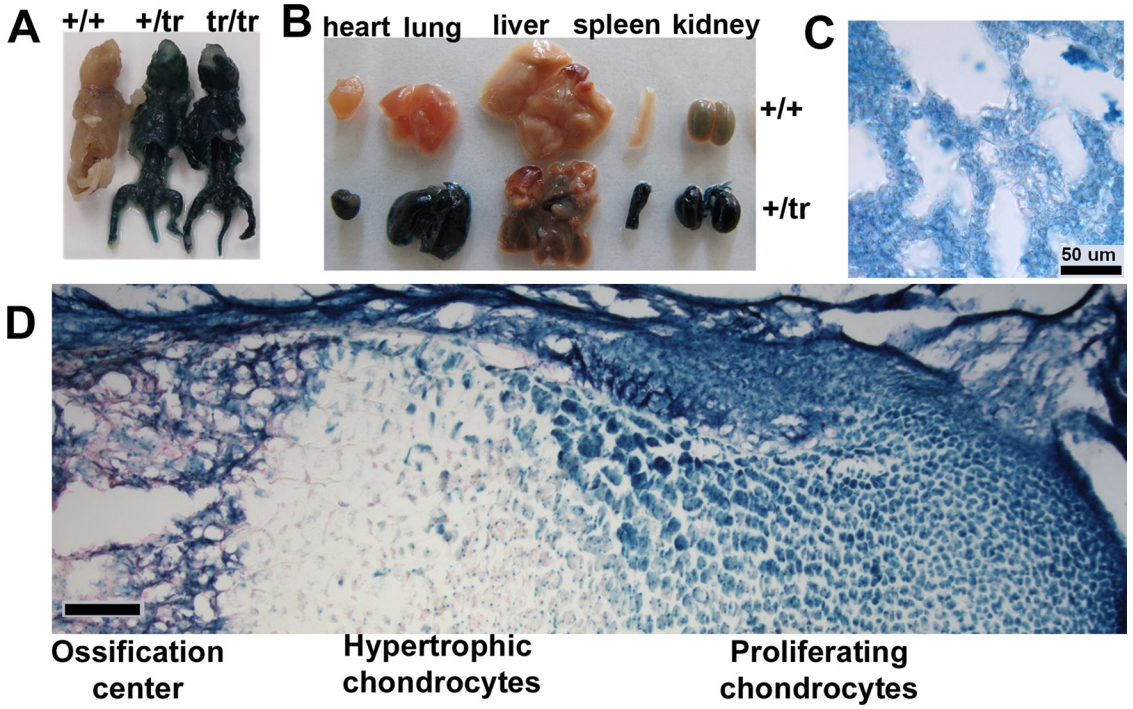


FIGURE 2: Examination of *Mex3c* expression in newborn mice by tracing β-gal activity. (A) High β-gal activity was detected in skeletal muscle. Bodies of 1-d-old pups were eviscerated followed by whole-mount X-Gal staining. The muscle tissues of +/tr and tr/tr pups were strongly positive for β-gal activity. The residual skin around the mouth and paws was negative, demonstrating the specificity of the staining. (B) Detecting β-gal activity in internal organs of newborn mice. β-Gal activity was high in most internal organs except for the liver. (C) All cells in the lung of newborn pups were β-gal positive. Scale bar: 50 μm. (D) Detecting β-gal activity in tibia of newborn mice. Cryosections of the proximal ends of tibia from +/tr mice were stained by X-Gal, followed by eosin counterstaining. Scale bar: 100 μm.

and bone in normal respiration, *Mex3c* expression was further examined by tracing β-gal activity on cryosections from 1-d-old pups. β-Gal activity was observed in all cell types in the lung (Figure 2C). In the developing tibia bone, resting and proliferating chondrocytes showed high β-gal activity, whereas hypertrophic chondrocytes showed low activity, and cells in the ossification center showed intermediate β-gal activity (Figure 2D). High *Mex3c* expression in the skeleton and lung may underlie perinatal lethality in *Mex3c* mutant mice, but the mechanism warrants further study. Adult *Mex3c* mutant mice were deficient in IGF1 (see later in the text), and IGF1 deficiency causes perinatal lethality because of poor respiration (Liu *et al.*, 1993; Govoni *et al.*, 2007b). Thus it is likely that perinatal lethality in *Mex3c* mutant mice is also related to IGF1 deficiency.

### Postnatal growth retardation in *Mex3c* mutant mice

In a mixed B6/129 or a mainly FVB/N background, more than 80% of tr/tr mice lived to adulthood. Mutant mice from these backgrounds were growth retarded, however, and had an average of 87% normal body length at various time points (Table 1). The few tr/tr mice of mainly C57/BL6 background which survived to adulthood were also growth retarded (unpublished data). Heterozygous mice showed normal growth. Consistent with reduced body length in tr/tr mice, tibias from mutant mice were also, on average, 15% shorter (unpublished data).

Histological analysis of tibial proximal growth plates from 20-d-old mutant mice, when the epiphyseal growth plate is most actively proliferating (Walker and Kember, 1972), revealed that the length of the growth plate was significantly decreased in mutant mice (Table 2). Although the lengths of the resting and the proliferating zones were not different between control and tr/tr mutant mice, that of the hypertrophic zone was significantly decreased in mutant mice (Table 2; Figure 3, A and B). Consistent with the attenuated hypertrophic zone, the mean height of terminal hypertrophic chondrocytes in mutant mice was significantly decreased (Table 2). In addition, a trend

| | Body length, cm; mean ± SEM (sample number) | | | | |
|---|---|---|---|---|---|
| Mice (age) | +/+ | +/– | –/– | Background | p Value |
| Female (4 wk) | 7.51 ± 0.15 (6) | N/A | 6.48 ± 0.28 (5) | Mixed[a] | <0.01 |
| Female (5 mo) | 9.80 ± 0.12 (8) | N/A | 8.44 ± 0.11 (5) | FVB | <0.0001 |
| Male (8 wk) | 9.58 ± 0.16 (10) | N/A | 8.38 ± 0.28 (9) | Mixed[a] | <0.001 |
| Male (6 wk) | 9.39 ± 0.08 (15) | 9.40 ± 0.08 (13) | 8.13 ± 0.24 (6) | FVB | <0.0001[b] |

[a]A mixed background between 129Sv and C57/BL6. [b]p values between +/+ versus –/–, and +/– versus –/– were both <.0001. There was no difference between +/+ and +/–.

TABLE 1: Mutant mice have reduced body length.

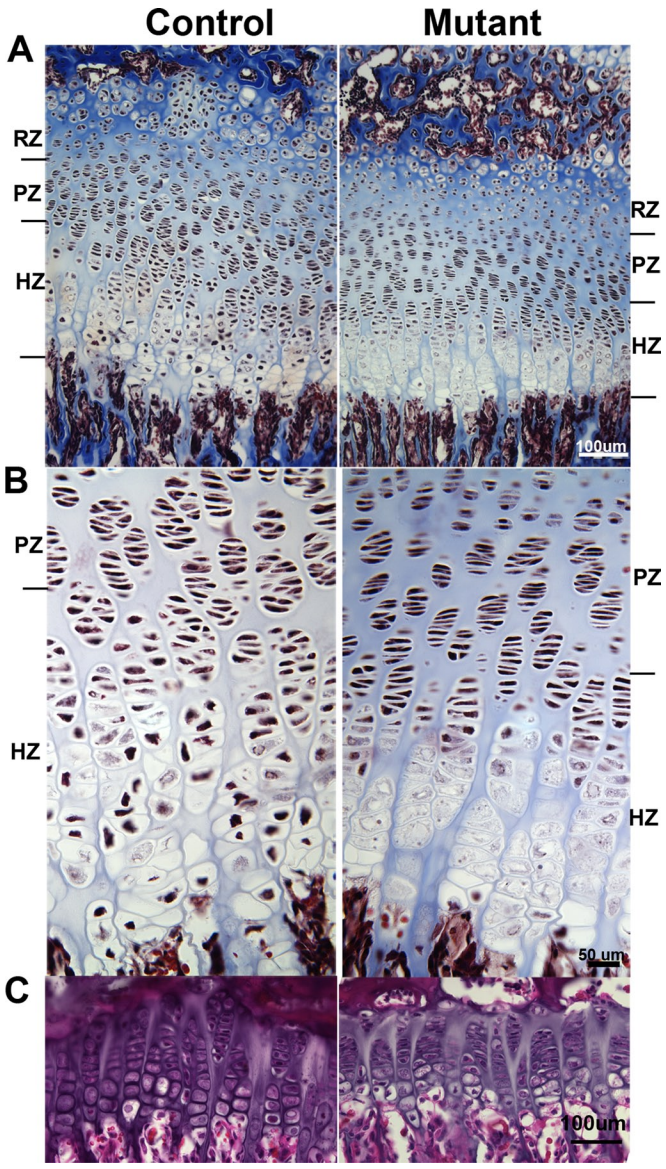


FIGURE 3: Analysis of growth plates from control and *Mex3c* mutant mice. (A) Proximal tibia growth plates of 20-d-old control and mutant mice. The hypertrophic zone (HZ), but not the resting zone (RZ) or the proliferating zone (PZ), was attenuated in the mutants. (B) High magnification showing the hypertrophic zone from (A). For (A) and (B), Masson's trichrome staining was performed on tibia sections from 20-d-old mice. (C) Growth plates of 8-wk-old control and mutant mice. Shown were hematoxylin and eosin–stained sections of proximal tibia. Scale bars in A and C equal 100 μm; in B, 50 μm.

of increasing cell size in cells between the proliferating chondrocytes and terminal chondrocytes was evident in control mice, but not in mutants (Figure 3B). At the age of 8 wk, most cells in the growth plate of control mice were undergoing hypertrophy, whereas in the growth plate of mutant mice, there were still chondrocytes in prehypertrophic stages (Figure 3C). The data suggest that chondrocyte hypertrophy is impaired in the mutant mice, and this impairment most likely underlies their postnatal growth retardation.

### IGF1 deficiency in *Mex3c* mutant mice

Because of the importance of the GH/IGF1 axis in postnatal growth control, we examined blood GH and IGF1 concentrations in mutant mice. Circulating GH concentrations of adult mutant mice were significantly higher than those of control mice (Table 3). Circulating IGF1 concentrations in mutant mice, however, were 40% lower than in normal mice (Table 3). IGF1 deficiency causes growth retardation in mice (Liu *et al.*, 1993; Powell-Braxton *et al.*, 1993) and impairs chondrocyte hypertrophy (Wang *et al.*, 1999). Sixty percent of normal serum IGF1, however, would be sufficient to maintain normal postnatal growth in *Mex3c* mutant mice if their local IGF1 production in the bone were unaffected (Sjogren *et al.*, 1999; Yakar *et al.*, 1999; Govoni *et al.*, 2007a, 2007b). IGF1 concentrations in bone (tibia and femur) extracts were compared by enzyme-linked immunosorbent assay (ELISA). IGF1 levels in extracts from mutant mice were found to be 42% lower than that of normal mice (Table 3), confirming IGF1 deficiency in bone.

Immunohistochemical analysis of developing bone revealed that in 20-d-old mutant mice, IGF1 protein was significantly decreased in resting and proliferating chondrocytes (Figure 4B, middle and right panels). The specificity of the signal was confirmed by the blocking peptide to significantly reduce the staining in these cells (Figure 4, left panel). The addition of blocking peptide only slightly decreased the signals in hypertrophic chondrocytes (Figure 4C), which could be the result of high IGF1 expression in hypertrophic chondrocytes (Gil-Pena *et al.*, 2009). IGF1 expression in cells of primary spongiosa of the mutant mice was also significantly reduced (Figure 4D). These observations were reproducible in tibia growth plates of multiple pairs of control and mutant mice and corroborated with our ELISA data that bone-forming cells from mutant mice produced reduced IGF1. These data confirmed IGF1 deficiency in bones of mutant mice. Thus we observed bone IGF1 deficiency and postnatal growth retardation in *Mex3c* mutant mice.

| | Control | Mutant | p Value |
|---|---|---|---|
| Growth plate (μm) | 370.7 ± 29.4 | 294.0 ± 27.4 | <0.05 |
| RZ (μm) | 24.5 ± 2.8 | 27.6 ± 2.2 | ns |
| PZ (μm) | 97.3 ± 10.0 | 100.0 ±12.2 | ns |
| HZ (μm) | 249.0 ± 23.2 | 166.4 ±18.0 | <0.05 |
| HZ cell height (μm) | 21.7 ± 0.5 | 17.5 ± 0.4 | <0.0001 |

Data are means ± SEM for five 20-d-old mice per group. Control mice included three +/+ mice and two +/tr mice. Values represent the longitudinal dimension of the structure parallel to the long axis of the bone. Twenty terminal chondrocytes from each of the five mice were measured to obtain the mean of HZ cell height.

TABLE 2: Growth plate parameters in control and tr/tr mice.

### *Mex3c* is highly expressed in the testis, ovary, brain, and developing bone

The expression of *Mex3c* in tissues of 4-wk-old mice was examined by tracing the activities of β-gal. *Mex3c* was highly expressed in the testis and the brain, but low in other internal organs, including the liver (Figure 5A). This finding was also confirmed by qRT-PCR, with the liver showing the lowest *Mex3c* expression among all the tissues examined (Figure 5B). Although *Mex3c* is highly expressed in the testis, *Mex3c* mutant males had normal spermatogenesis and were fertile with normal litter size. *Mex3c* was also readily detected in the female reproductive system including the ovary, the uterus, and the oviducts (Figure 5A). Mutant females, however, were also fertile, although they tended to have their first litters 2–3 wk later than do normal mice, which might be the result of growth retardation. Because there is still a low level (2%) of authentic *Mex3c* mRNA in

| | | Mean ± SEM (sample number) | | | |
|---|---|---|---|---|---|
| | Mice (age) | Control | Mutant | Background | p Value |
| GH (ng/ml) | Male (8 wk) | 4.89 ± 1.56 (11)[a] | 11.84 ± 2.67 (11) | Mixed[b] | <0.05 |
| Serum IGF1 (ng/ml) | Female (2–3 mo) | 590.7 ± 32.08 (10) | 342.8 ± 37.19 (10) | FVB | <0.0001 |
| | Male (5 mo) | 407.7 ± 16.87 (18) | 262.5 ± 25.02 (13) | FVB | <0.0001 |
| Bone IGF1 (pg/mg bone) | Female (6–7 wk) | 134.3 ± 11.02 (6) | 77.54 ± 15.11 (5) | FVB | <0.05 |

[a]Control mice for GH measurement included +/+ and +/tr mice; control mice for IGF1 assays were all +/+ mice. [b]A mixed background between 129Sv and C57/BL6.

TABLE 3: Mutant mice have abnormal GH and IGF1 levels.

homozygous mutant mice, the residual MEX3C protein might have been enough to maintain normal gametogenesis in both sexes. A null *Mex3c* mutant is thus needed to test whether *Mex3c* is necessary for normal reproduction. Consistent with high *Mex3c* expression in the brain, we found that mutant mice had reduced fat deposition related to abnormal energy expenditure (unpublished observation).

Chondrocyte hypertrophy is apparently affected in *Mex3c* mutant mice; thus we examined *Mex3c* gene expression in the growth plates of developing tibias. *Mex3c* was highly expressed in chondrocytes of the resting and proliferating zones (Figure 5C). In the hypertrophic zone, *Mex3c* showed decreased expression, and β-gal activity was barely detectable in fully hypertrophic chondrocytes. *Mex3c* expression was high in stromal cells in the matrix of spongy bone (Figure 5D) and compact bone (Figure 5E). Strong β-gal activity was also observed in periosteum, a membrane structure generating osteoblasts. Comparing the pattern of IGF1 deficiency and *Mex3c* expression in the growth plate, IGF1 deficiency was pronounced in cells of mutant mice that normally had high *Mex3c* expression. MEX3C is an intracellular RNA-binding protein; high expression of *Mex3c* in multiple types of bone cells suggests that IGF1 deficiency in these cells of mutant mice could be a direct effect of MEX3C deficiency. The data also suggest that *Mex3c* mutation has varied effects on organs with high *Mex3c* expression.

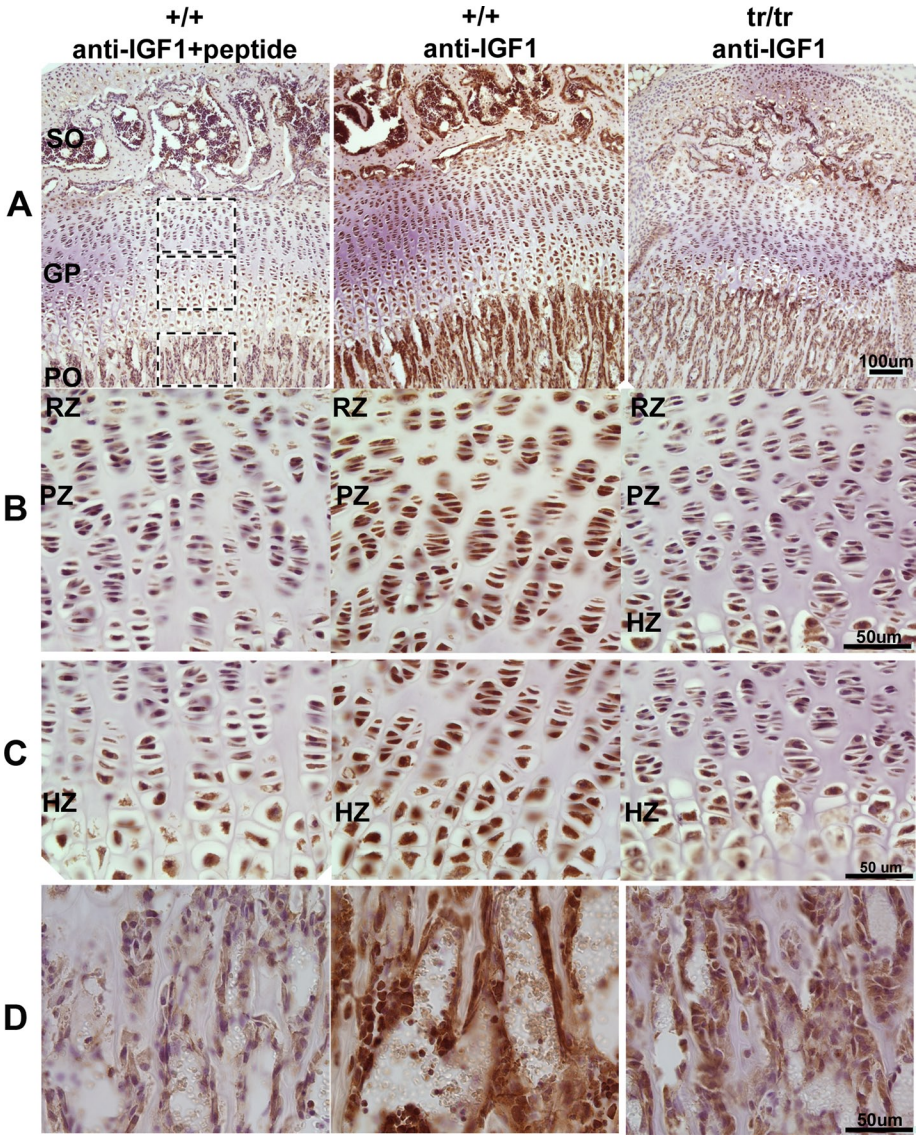


FIGURE 4: Reduced IGF1 expression in bone cells of *Mex3c* mutant mice. (A) IGF1 immunohistochemical analysis of proximal tibia growth plates (GPs) of 20-d-old mice. The three boxes indicate the areas shown in B, C, and D. (B) High magnification showing the proliferating zone (PZ) of the growth plate. (C) High magnification showing the hypertrophic zone (HZ) of the GP. (D) High magnification of the spongiosa region. SO, secondary ossification center; PO, primary ossification center.

### IGF1 deficiency in *Mex3c* mutant mice is not caused by decreased *Igf1* mRNA level

qRT-PCR revealed that total *Igf1* transcripts (including those with short and long 3′ UTRs) in tissues (such as the liver, kidney, spleen, and testis) and muscle from mutant mice were not significantly decreased (Figure 6A). Although the liver and kidney of mutant mice showed 23% less expression of *Igf1* mRNA, this marginal decrease did not account for the 40% reduction in serum IGF1 levels, because serum IGF1 levels that were 71% of normal levels were observed in animals with 28% of normal levels of the 1-kb short-form *Igf1* transcripts and 52% of normal levels of 7-kb long-form *Igf1* transcripts (Liu *et al.*, 1998). Cells in tibia from mutant mice were clearly deficient in IGF1 protein.

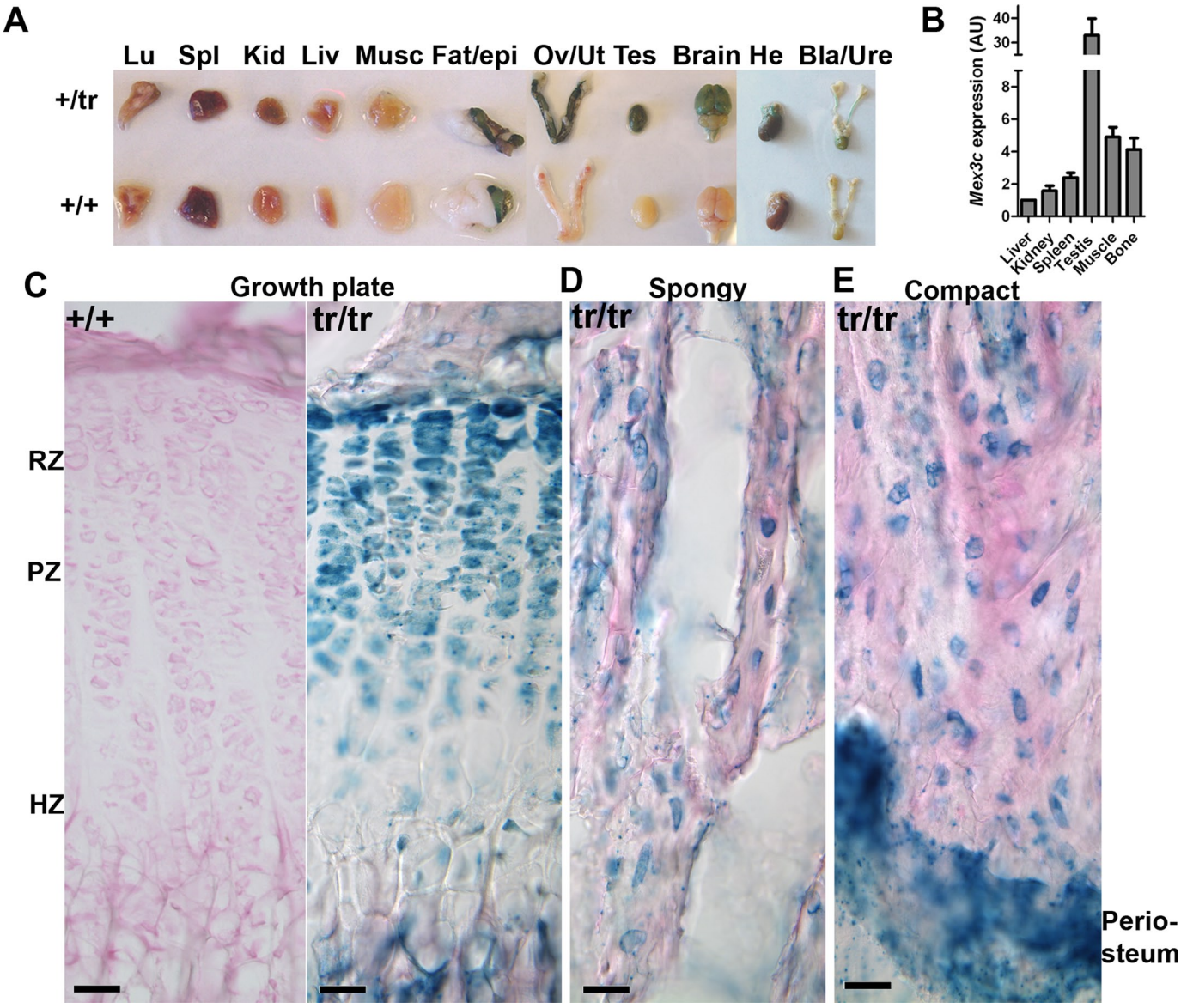


FIGURE 5: Analysis of *Mex3c* expression in mouse tissues. (A) Expression of *Mex3c* in tissues of developing mice. Tissues from 4-wk-old heterozygous and normal mice were stained for β-gal; positive tissues were stained blue. The epididymis were positive even in normal mice (+/+) due to endogenous β-gal activity, which indicates the reliability of the staining condition. Lu: lung; Spl: spleen; Kid: kidney; Liv: liver; Musc: skeletal muscle; Fat/epi: gonadal fat/epididymis; Ov/Ut: ovary/uterus; Tes: testis; He: heart; Bla/Ure: bladder/ureter. (B) qRT-PCR analysis of *Mex3c* mRNA in various tissues from normal mice. Means ± SEM of data from four mice are presented. (C) *Mex3c* expression in chondrocytes of proximal tibia growth plates of 20-d-old mice indicated by tracing β-gal activity. β-Gal–positive cells were stained blue. No β-gal–positive cells were observed in control (+/+) mice. The sections were counterstained with eosin to show the matrix in red. RZ, resting zone; PZ, proliferating zone; HZ, hypertrophic zone. (D) Expression of *Mex3c* in stromal cells of the spongy bone. (E) Expression of *Mex3c* in stromal cells of the compact bone. Scale bars: 50 μm.

qRT-PCR analysis found that *Igf1* mRNA levels in tibias of mutant mice were not different from those of controls (Figure 6B), demonstrating that IGF1 deficiency in *Mex3c* mutant mice was not caused by decreased *Igf1* mRNA levels. Thus our data suggest that MEX3C deficiency most likely affected *Igf1* mRNA translation, but not *Igf1* mRNA transcription or turnover.

### MEX3C enriched *Igf1* mRNA from tissue lysates

MEX3C has two KH RNA-binding domains; we examined whether MEX3C interacted with *Igf1* mRNA. Glutathione *S*-transferase (GST), GST-MEX3C, GST-MEX3C/C (GST fused to the C-terminal 263 AA of MEX3C which contains the ZNF domain but not the two KH RNA-binding domains; Figure 6C), and GST-MEX3C/N (GST fused to the N-terminal 296 AA of MEX3C, containing the two KH RNA-binding domains but not the ZNF domain) were tested for their capability to enrich *Igf1* mRNA from brain lysate. We chose the brain because it expresses *Igf1* and has high *Mex3c* expression. qRT-PCR revealed that GST-MEX3C and GST-MEX3C/N pulled down significantly more *Igf1* mRNA than did GST and GST-MEX3C/C, which lack RNA-binding domains (Figure 6D). Although mRNA of *Gapdh* and all five other mRNA species tested were also enriched by GST-MEX3C and GST-MEX3C/N (unpublished data), their enrichment was all KH

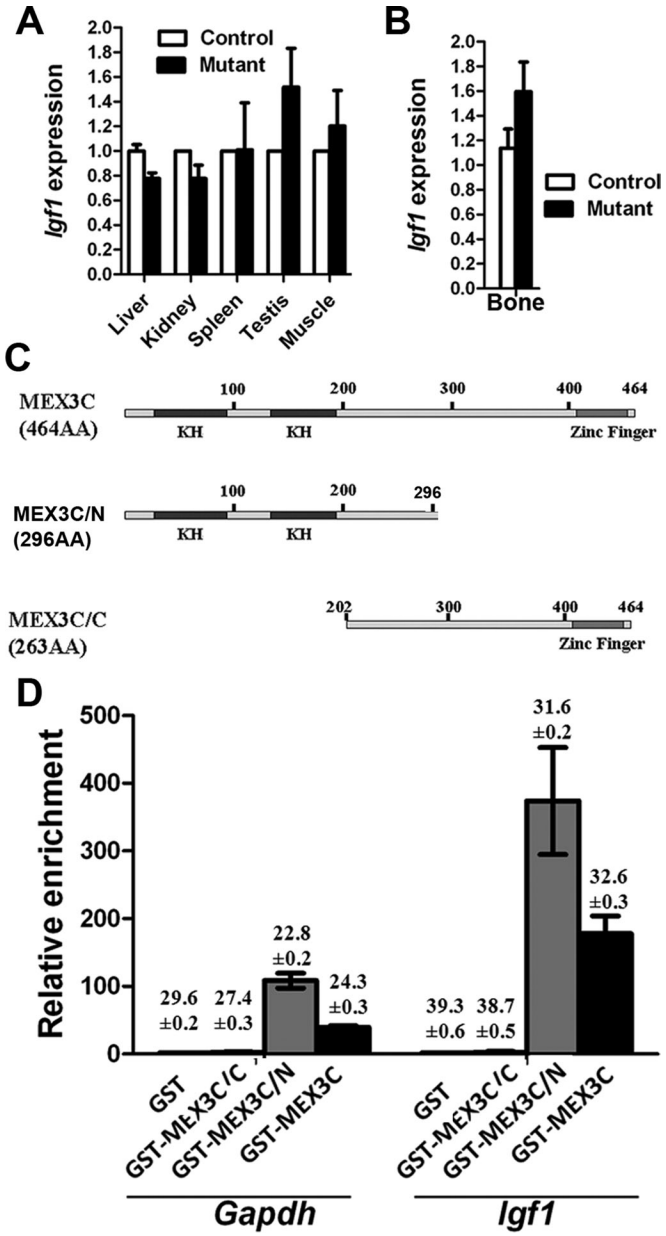


FIGURE 6: qRT-PCR analysis of *Igf1* mRNA in mutant mice and in GST pull-down assays. (A) Comparison of *Igf1* mRNA levels in liver, kidney, spleen, testis, and muscle tissues from +/+ and tr/tr mice. Four 4~5-wk-old male mice for each genotype were analyzed. Expression in tissues of control mice was set as 1. Means ± SEM are presented. (B) *Igf1* mRNA expression in +/+ and tr/tr tibia. (C) Diagram showing domains in MEX3C, MEX3C/N, and MEX3C/C. KH: KH RNA-binding domain. (D) GST pull-down analysis of *Igf1* mRNA enrichment by partial and full-length MEX3C proteins. Means ± SEM of three independent assays are presented. mRNA levels in GST-only assays were set as 1. Numbers above the columns are means ± SEM of Ct numbers.

domain-dependent. The sequence of *C. elegans* MEX-3 recognition element (MRE) was defined as (A/G/U)(G/U)AGN(0–8)U(U/A/C)UA) and was found in the 3′-UTR of ~26.2% of all genes in *C. elegans* (Pagano *et al.*, 2009). Considering genes with this MRE in the 5′-UTR and coding region, a higher proportion of *C. elegans* mRNA is expected to contain this MRE and bind MEX-3. Thus MEX-3 is able to bind multiple mRNA species. The KH RNA binding domains of mouse MEX3C are nearly 90% identical to *C. elegans* MEX-3 KH domains. This high identity suggests that mouse MEX3C might also interact with multiple mRNA molecules. Indeed, human MEX3C is able to associate with poly(A), poly(U), and multiple mRNA species (Buchet-Poyau *et al.*, 2007). Whether *Igf1* mRNA interacts directly with MEX3C is still an open question, however.

## DISCUSSION

Here we report that *Mex3c* mutant mice showed growth retardation, background-dependent perinatal lethality, and IGF1 deficiency. Although MEX3C deficiency also affects energy balance and decreases fat deposition, rescuing the slim phenotype by introducing an ob/ob mutation did not rescue growth retardation (our unpublished data), excluding the possible effects of negative energy balance on postnatal growth. We postulate that IGF1 deficiency might be a major mechanism underlying the phenotypes in the mutants described in this work.

Eighty-five percent of *Mex3c* mutant mice in the C57BL/6 background died from poor respiration soon after birth, similar to knockout mouse models deficient in IGF1 signaling. Constitutive *Igf1* knockout causes background-dependent perinatal lethality (Liu *et al.*, 1993), and osteoblast-specific *Igf1* knockout causes similar postnatal death (Govoni *et al.*, 2007b). In both cases, poor breathing was the cause of death. We did not examine whether IGF1 was deficient in newborn mutant pups. Because *Mex3c* is highly expressed in multiple tissues of newborn pups, and IGF1 deficiency is observed in adult mutant mice, IGF1 deficiency could also be present in newborn pups, and this could underlie their perinatal lethality.

Although serum IGF1 levels in *Mex3c* mutant mice are 60% of normal levels and by themselves do not account for postnatal growth retardation, we observed local IGF1 deficiency in the bone. Chondrocyte- and osteoblast-specific *Igf1* knockout affects postnatal growth even though circulating IGF1 levels are normal (Govoni *et al.*, 2007a, 2007b). Thus local deficiency of IGF1 in the bone of *Mex3c* mutant mice might underlie the observed attenuated growth. Consistent with local deficiency of IGF1 in *Mex3c* mutant mice, *Mex3c* is highly expressed in resting and proliferating chondrocytes, as well as in bone stromal cells. Our analysis of growth plate from *Mex3c* mutant mice showed that chondrocyte hypertrophy was affected, the same phenomenon noted in *Igf1* mutant mice (Wang *et al.*, 1999). Thus our data suggest that IGF1 deficiency most likely underlies the growth retardation observed in *Mex3c* mutant mice.

Although a specific MEX3C antibody is unavailable to confirm MEX3C deficiency at the protein level, the finding that tr/tr mice have only 2% normal *Mex3c* mRNA expression suggests that MEX3C protein deficiency is highly likely. Although the possibility of toxic gain of function of MEX3C-β-gal fusion protein cannot be excluded at the moment, its likelihood is low. So far, nearly 1000 articles have been published describing various phenotypes of gene trap mice, and many of these mice express a fusion protein from the trapped host gene and the reporter LacZ. To the best of our knowledge, toxic gain of function of the host peptide-β-gal fusion protein has not been reported to account for the observed phenotypes. In addition, *Mex3c* is highly expressed in the testis, ovary, and brain; the toxic effects would also be evident in these organs if MEX3C-β-gal is indeed a toxic protein. Mutant mice, however, have normal gametogenesis and are fertile. Although tr/tr mice showed abnormal energy expenditure and reduced fat deposition, tr/tr;ob/ob double mutant mice were obese but still growth retarded (our unpublished observations), excluding a role of energy expenditure on growth.

The tissue- and pathway-specific effects of *Mex3c* mutation also argue against the possibility of a toxic gain-of-function mechanism in the growth retardation of tr/tr mice.

*Igf1* mRNA was decreased by 23% in the liver and the kidney of *Mex3c* mutant mice but not in the other organs, including the bone. Although it is unclear why *Igf1* transcription is not increased in the mutants, which had higher levels of GH than did control mice, the marginal decrease of *Igf1* mRNA in the liver and the kidney could be indirect effects of MEX3C deficiency, because *Mex3c* has relatively low expression in these two organs. Neither the 40% decrease of circulating IGF1 nor the decrease of local IGF1 production in the bone of mutant mice can be explained by decreased *Igf1* mRNA levels. Although deficiency of acid-labile subunit and IGF binding proteins leads to decreased circulating IGF1 (Ueki *et al.*, 2000; Ning *et al.*, 2006), this deficiency does not cause perinatal lethality or dramatic growth retardation. In addition, deficiency of these proteins does not decrease local expression of IGF1 in bone. IGF1 production must have been affected in *Mex3c* mutant mice. Our data suggest that, although MEX3C deficiency may not affect *Igf1* mRNA transcription or stability, it most likely affects *Igf1* expression at the protein level.

MEX3C protein is an RNA-binding protein and contains two KH-type RNA-binding domains and one ZNF domain mediating protein–protein interaction. GST pull-down assays showed that GST-MEX3C and GST-MEX3C/N (the N-terminal MEX3C containing two RNA-binding domains) pulled down 200- and 400-fold more *Igf1* mRNA from mouse brain lysate than did GST, demonstrating that the MEX3C N terminus containing the RNA-binding domains is necessary and sufficient to enrich *Igf1* mRNA. We noted that in this GST pull-down assay, GST-MEX3C and GST-MEX3C/N were able to enrich all the mRNA species we had tested to various degrees, reminiscent of human MEX3C, which associates with poly(A), poly(U), and multiple mRNA species including *Gapdh* (Buchet-Poyau *et al.*, 2007). *C. elegans* MEX-3 binds to a consensus MRE which is present in a large proportion of *C. elegans* genes (Pagano *et al.*, 2009). Thus our observation that MEX3C, a MEX-3 homologue, can pull down multiple mRNAs including *Igf1* mRNA from mouse tissue lysates is not surprising. We noted that the C terminus of MEX3C showed inhibitory effects on RNA pull-down. It is likely that the C terminus of MEX3C provides a mechanism for mRNA selectivity. Although it remains to be determined whether *Igf1* mRNA is a direct or an indirect target of MEX3C and the region of *Igf1* mRNA necessary for the interaction, our data suggest that *Igf1* mRNA could be an mRNA target for MEX3C.

MEX3C's *C. elegans* homologue MEX-3 repressed the translation of *pal-1* and nanos mRNA through unknown mechanisms (Draper *et al.*, 1996; Hunter and Kenyon, 1996; Jadhav *et al.*, 2008). Our data suggest that MEX3C deficiency inhibits the translation of *Igf1* mRNA. Bone-forming cells express predominantly *Igf1* transcripts of ~7000 nt with a long 3′ UTR (Delany and Canalis, 1995), and, in the liver, *Igf1* transcripts with a long 3′-UTR have low translatability (Foyt *et al.*, 1991). Local production of IGF1 in the bone is essential for normal postnatal growth (Govoni *et al.*, 2007a, 2007b). We propose that *Igf1* mRNA with a long 3′-UTR may need *trans*-acting factors to improve their translatability in bone-forming cells, and MEX3C or its interacting partner could be one of these *trans*-acting factors. This proposal would explain why *Mex3c* mutation impairs bone IGF1 production and postnatal growth. Our data and those of others suggest that MEX3C seems able to bind multiple mRNA molecules. How *Mex3c* mutation affects the translation of certain mRNA molecules, such as *Igf1* mRNA, but not others needs further study. In summary, our data suggest that MEX3C plays an important role in enhancing the translation of *Igf1* mRNA directly or indirectly and promoting postnatal growth.

## MATERIALS AND METHODS

### Generation of *Mex3c* gene trap mice

The *Mex3c* gene trap ES cell line DD0642 was obtained from the Sanger Institute Gene Trap Resource (SIGTR, Cambridge, UK). The ES cells were microinjected into mouse blastocysts, and the resulting chimera males were mated with C57/BL6 females to obtain heterozygous *Mex3c* gene trap mice. Heterozygous mice were intercrossed to obtain mutant mice of 129Sv/C57 mixed background. Heterozygous mice were backcrossed to C57/BL6 or FVB/N for six generations to obtain mutant mice of mainly C57/BL6 or FVB/N background. Mice were housed in the animal facility of Wake Forest University Health Sciences (Winston-Salem, NC). Experiments were conducted in accordance with the National Research Council publication *Guide for the Care and Use of Laboratory Animals*, and were approved by the Institutional Animal Care and Use Committee of Wake Forest University. Mice were kept in microisolator cages with 12-h light/dark cycles and were fed ad libitum. A chow diet (Prolab, RMH3000; PMI Nutrition International, Henderson, CO) was used for colony maintenance.

### Genotyping

Ear biopsies were lysed as previously described for genotyping (Agoulnik *et al.*, 2002). The gene trap allele was detected by PCR amplification of a 419–base pair product with primer TrapF (ttcaacatcagccgctacag) and TrapR (ctcgtcctgcagttcattca). Homozygous gene trap mice were distinguished from heterozygous mice by PCR with primer pair D18Mit210F (tgggcagaagtataactaaatcca) and D18Mit210R (ttcaaaccgtatgcctttcc). The thermal cycle parameters were: 94°C 4 min, followed by 35 cycles of 94°C, 30 s; 55°C, 30 s; 72°C, 30 s. A 122–base pair PCR product was obtained from the C57BL/6 and FVB alleles, and a 146–base pair PCR product was obtained from the gene trap 129/Sv allele. The size difference was resolved on a 3% agarose gel stained with ethidium bromide.

### Expression and purification of GST fusion proteins

*Escherichia coli* BL21(DE3) transformed with plasmid DNA (pGEX4T1, pGEX4T1/MEX3C, pGEX4T1/MEX3C/C, and pGEX4T1/MEX3C/N) was used for GST fusion expression as described (Zhou *et al.*, 2005). Glutathione sepharose 4B beads (GE Life Sciences, Pittsburgh, PA) were used to purify the GST fusion proteins according to the manufacturer's instructions.

### GST pull-down assay

GST pull down and immunoprecipitation were performed as described (Lu and Bishop, 2003; Zhang *et al.*, 2005). The final precipitates were either lysed in 50 µl of 1X SDS loading buffer for SDS–PAGE and Western blotting analysis or used for RNA extraction using the RNeasy Protect kit (QIAGEN, Valencia, CA) for qRT-PCR analysis.

### qRT-PCR

Mice were killed by $CO_2$ overdose, and tissues were snap frozen in liquid nitrogen and then stored at –80°C before RNA extraction. To extract RNA from developing tibia, all muscle tissue was removed from the bone, and the bone marrow cells were removed by several flushes with ice-cold phosphate-buffered saline (PBS) solution. Then bones were ground in liquid nitrogen, and RNA was extracted from bone powders with TRIzol (Invitrogen, Life Technologies, Grand Island, NY). Total RNA from soft tissues was extracted with an RNeasy Mini Kit (QIAGEN) as instructed by the manufacturer. Reverse

transcription was performed with the SuperScript First-Strand Synthesis System from Invitrogen.

Real-time PCR was performed on a 7300 real-time PCR system (Applied Biosystems, Foster City, CA). For mouse *Gapdh*, *Hprt1*, and *Igf1*, TaqMan probes (Applied Biosystems) were used. The *Igf1* Taqman probe recognizes both the short form and long forms of *Igf1* transcripts. For *Mex3c* (*Mex3cF*: atgctgtcccacgcctac, and *Mex3cR*: agtgctttaattttacaaccctgg) and *Ppib* (*PpibF*: tcgtctttggactctttggaa and *PpibR*: agcgctcaccatagatgctc) real-time PCR, SYBR Green PCR Master Mix (Applied Biosystems) was used. After the PCR amplification, a dissociation program was run, and the amplified product was analyzed by electrophoresis to verify the specificity of the amplification. Relative gene expression levels were calculated using the CT method (Livak and Schmittgen, 2001). In cases where mRNA was not detected after 40 cycles, the cycle threshold (Ct) number was set as 40 for analysis. Three to five animals were assayed for each group. Three independent experiments were performed with each experiment performed in triplicate. Results were presented as mean ± SEM.

### Growth plate analysis

Tibias from newborn, 20-d-old, and 8-wk-old mice were fixed in 4% paraformaldehyde (PFA)/PBS at 4°C for 4 h. Bones from 20-d-old and 8-wk-old mice were decalcified in Immunocal (Decal Chemical, Tallman, NY) at 4°C for 30 min to 1 h. Bones were dehydrated and embedded in paraffin to obtain paraffin sections for hematoxylin and eosin staining or Masson's trichrome staining.

The longitudinal dimensions of the proximal tibial growth plate and the heights of terminal chondrocytes were measured on photomicrographs of anatomically matched midsagittal sections, taken under a 20× objective with an Axio M1 microscope and an AxioCam MRc digital camera (Carl Zeiss, Thornwood, NY). Measurements were performed with ImageJ software.

### Immunostaining of tibia sections

For histochemical analysis, decalcified bones were immersed in 30% sucrose/PBS overnight at 4°C before they were embedded in optimal cutting temperature (OCT) compound for cryosectioning. To examine the expression of *Mex3c* through detecting β-gal activity, bone cryosections were stained with X-GAL as described (Beddington *et al.*, 1989). To examine the expression of IGF1 in the bone, bone cryosections were fixed with 4% PFA, and treated with 3% $H_2O_2$/PBS for 30 min to inactivate endogenous peroxidase activity. Then the sections were blocked with Protein Block (Dako, Carpinteria, CA) for 1 h, and incubated with anti-IGF1 antibody (Santa Cruz Biotechnology, Santa Cruz, CA; 1:100) at 4°C overnight. To confirm specificity, anti-IGF antibody was preincubated with a fivefold concentration of IGF1 blocking peptide (Santa Cruz Biotechnology) for 2 h before the antibody was applied to the sections. After three 5-min washes in Tris-buffered saline and Tween 20 (TBS/T), the sections were incubated with biotin-conjugated anti-goat secondary antibody (1:300; Vector Labs, Burlingame, CA) at room temperature for 1 h. Then the sections were washed in TBS/T three times and were incubated for 30 min with ABS reagents (Vector Labs). After three 5-min washes, the signals were visualized by ImmPACT DAB (Vector Labs). The sections were counterstained with hematoxylin before mounting. Images were taken with an Axio M1 microscope equipped with an AxioCam MRc digital camera (Carl Zeiss).

### Hormone and growth factor assays

Serum was obtained from the saphenous vein of mice at ages listed in Table 1. GH was assayed with the mouse/rat GH ELISA kit purchased from Millipore (cat. EZRMGH-45K; Billerica, MA) as instructed by the manufacturer. Serum IGF1 was assayed with a mouse/rat IGF1 immunoassay kit from R&D Systems (Minneapolis, MN). To assay IGF1 in bone extracts, tibia and femur bones were rid of muscle tissues manually. Bones were homogenized with a motor homogenizer in RIPA buffer (1 g of bone in 5 ml of buffer), and lysates were incubated with shaking at 4°C for 1 h. The lysates were centrifuged at 12,000 *g* at 4°C for 10 min. The cleared supernatants were diluted 20 times for the ELISA.

## ACKNOWLEDGMENTS

We thank Karen Klein (Research Support Core, Office of Research, Wake Forest University Health Sciences) for editing the manuscript. This work was supported by the National Institutes of Health (U01HD043421 to C.B., R01HD058058 to B. L.).

## REFERENCES

Agoulnik AI, Lu B, Zhu Q, Truong C, Ty MT, Arango N, Chada KK, Bishop CE (2002). A novel gene, Pog, is necessary for primordial germ cell proliferation in the mouse and underlies the germ cell deficient mutation, gcd. Hum Mol Genet 11, 3047–3053.

Beddington RS, Morgernstern J, Land H, Hogan A (1989). An in situ transgenic enzyme marker for the midgestation mouse embryo and the visualization of inner cell mass clones during early organogenesis. Development 106, 37–46.

Bell GI, Stempien MM, Fong NM, Rall LB (1986). Sequences of liver cDNAs encoding two different mouse insulin-like growth factor I precursors. Nucl Acids Res 14, 7873–7882.

Buchet-Poyau K, Courchet J, Hir HL, Seraphin B, Scoazec J-Y, Duret L, Domon-Dell C, Freund J-N, Billaud M (2007). Identification and characterization of human Mex-3 proteins, a novel family of evolutionarily conserved RNA-binding proteins differentially localized to processing bodies. Nucl Acids Res 35, 1289–1300.

Ciosk R, DePalma M, Priess JR (2006). Translational regulators maintain totipotency in the Caenorhabditis elegans germline. Science 311, 851–853.

Delany AM, Canalis E (1995). Transcriptional repression of insulin-like growth factor I by glucocorticoids in rat bone cells. Endocrinology 136, 4776–4781.

Donnini M, Lapucci A, Papucci L, Witort E, Jacquier A, Brewer G, Nicolin A, Capaccioli S, Schiavone N (2004). Identification of TINO: a new evolutionarily conserved BCL-2 Au-rich element RNA-binding protein. J Biol Chem 279, 20154–20166.

Draper BW, Mello CC, Bowerman B, Hardin J, Priess JR (1996). MEX-3 Is a KH domain protein that regulates blastomere identity in early C. elegans embryos. Cell 87, 205–216.

Foyt HL, LeRoith D, Roberts CT, Jr (1991). Differential association of insulin-like growth factor I mRNA variants with polysomes in vivo. J Biol Chem 266, 7300–7305.

Gil-Pena H, Garcia-Lopez E, Alvarez-Garcia O, Loredo V, Carbajo-Perez E, Ordonez FA, Rodriguez-Suarez J, Santos F (2009). Alterations of growth plate and abnormal insulin-like growth factor I metabolism in growth-retarded hypokalemic rats: effect of growth hormone treatment. Am J Physiol Renal Physiol 297, F639–F645.

Govoni KE, Lee SK, Chung YS, Behringer RR, Wergedal JE, Baylink DJ, Mohan S (2007a). Disruption of insulin-like growth factor-I expression in type IIalphal collagen-expressing cells reduces bone length and width in mice. Physiol Genomics 30, 354–362.

Govoni KE, Wergedal JE, Florin L, Angel P, Baylink DJ, Mohan S (2007b). Conditional deletion of insulin-like growth factor-I in collagen type 1alpha2-expressing cells results in postnatal lethality and a dramatic reduction in bone accretion. Endocrinology 148, 5706–5715.

Grishin NV (2001). KH domain: one motif, two folds. Nucl Acids Res 29, 638–643.

Guzman B, Cormand B, Ribases M, Gonzalez-Nunez D, Botey A, Poch E (2006). Implication of chromosome 18 in hypertension by sibling pair and association analyses: putative involvement of the RKHD2 gene. Hypertension 48, 883–891.

Hunter CP, Kenyon C (1996). Spatial and temporal controls target pal-1 blastomere-specification activity to a single blastomere lineage in C. elegans embryos. Cell 87, 217–226.

Jadhav S, Rana M, Subramaniam K (2008). Multiple maternal proteins coordinate to restrict the translation of C. elegans nanos-2 to primordial germ cells. Development 135, 1803–1812.

Kawai M, Delany AM, Green CB, Adamo ML, Rosen CJ (2010). Nocturnin suppresses igf1 expression in bone by targeting the 3′ untranslated region of igf1 mRNA. Endocrinology 151, 4861–4870.
Liu JL, Grinberg A, Westphal H, Sauer B, Accili D, Karas M, LeRoith D (1998). Insulin-like growth factor-I affects perinatal lethality and postnatal development in a gene dosage-dependent manner: manipulation using the Cre/loxP system in transgenic mice. Mol Endocrinol 12, 1452–1462.
Liu JP, Baker J, Perkins AS, Robertson EJ, Efstratiadis A (1993). Mice carrying null mutations of the genes encoding insulin-like growth factor I (Igf-1) and type 1 IGF receptor (Igf1r). Cell 75, 59–72.
Livak KJ, Schmittgen TD (2001). Analysis of relative gene expression data using real-time quantitative PCR and the 2-[Delta][Delta] CT method. Methods 25, 402–408.
Lu B, Bishop CE (2003). Mouse GGN1 and GGN3, two germ cell specific proteins from the single gene Ggn, interact with mouse POG and play a role in spermatogenesis. J Biol Chem 278, 16289–16296.
Lu B, Geurts AM, Poirier C, Petit DC, Harrison W, Overbeek PA, Bishop CE (2007). Generation of rat mutants using a coat color-tagged Sleeping Beauty transposon system. Mamm Genome 18, 338–346.
Ning Y, Schuller AG, Bradshaw S, Rotwein P, Ludwig T, Frystyk J, Pintar JE (2006). Diminished growth and enhanced glucose metabolism in triple knockout mice containing mutations of insulin-like growth factor binding protein-3, -4, and -5. Mol Endocrinol 20, 2173–2186.
Ohlsson C, Mohan S, Sjogren K, Tivesten A, Isgaard J, Isaksson O, Jansson JO, Svensson J (2009). The role of liver-derived insulin-like growth factor-I. Endocr Rev 30, 494–535.
Pagano JM, Farley BM, Essien KI, Ryder SP (2009). RNA recognition by the embryonic cell fate determinant and germline totipotency factor MEX-3. Proc Natl Acad Sci USA 106, 20252–20257.
Powell-Braxton L, Hollingshead P, Warburton C, Dowd M, Pitts-Meek S, Dalton D, Gillett N, Stewart TA (1993). IGF-I is required for normal embryonic growth in mice. Genes Dev 7, 2609–2617.
Rodriguez S, Gaunt TR, Day IN (2007). Molecular genetics of human growth hormone, insulin-like growth factors and their pathways in common disease. Hum Genet 122, 1–21.
Sjogren K *et al.* (1999). Liver-derived insulin-like growth factor I (IGF-I) is the principal source of IGF-I in blood but is not required for postnatal body growth in mice. Proc Natl Acad Sci USA 96, 7088–7092.
Skarnes WC *et al.* (2004). A public gene trap resource for mouse functional genomics. Nat Genet 36, 543–544.
Stratikopoulos E, Szabolcs M, Dragatsis I, Klinakis A, Efstratiadis A (2008). The hormonal action of IGF1 in postnatal mouse growth. Proc Natl Acad Sci USA 105, 19378–19383.
Ueki I, Ooi GT, Tremblay ML, Hurst KR, Bach LA, Boisclair YR (2000). Inactivation of the acid labile subunit gene in mice results in mild retardation of postnatal growth despite profound disruptions in the circulating insulin-like growth factor system. Proc Natl Acad Sci USA 97, 6868–6873.
Walker KV, Kember NF (1972). Cell kinetics of growth cartilage in the rat tibia. I. Measurements in young male rats. Cell Tissue Kinet 5, 401–408.
Wang J, Zhou J, Bondy CA (1999). Igf1 promotes longitudinal bone growth by insulin-like actions augmenting chondrocyte hypertrophy. FASEB J 13, 1985–1990.
Yakar S, Liu JL, Stannard B, Butler A, Accili D, Sauer B, LeRoith D (1999). Normal growth and development in the absence of hepatic insulin-like growth factor I. Proc Natl Acad Sci USA 96, 7324–7329.
Zhang J, Wang Y, Zhou Y, Cao Z, Huang P, Lu B (2005). Yeast two-hybrid screens imply that GGNBP1, GGNBP2 and OAZ3 are potential interaction partners of testicular germ cell-specific protein GGN1. FEBS Lett 579, 559–566.
Zhou Y, Zhao Q, Bishop CE, Huang P, Lu B (2005). Identification and characterization of a novel testicular germ cell-specific gene Ggnbp1. Mol Reprod Dev 70, 301–307.